Universität Hamburg
DER FORSCHUNG | DER LEHRE | DER BILDUNG

RD50

The boron-oxygen (B_iO_i) defect complex induced by irradiation with 23 GeV protons in p-type epitaxial silicon diodes

Chuan Liao[a], E. Fretwurst[a], E. Garutti[a], J. Schwandt[a], A Himmerlich[b], Y. Gurimskaya[b], I. Mateu[b], M. Moll[b], M. F. Garcia[c], L. Makarenko[d], I. Pintilie[e]
[a]Hamburg University (GE), [b]CERN (SW), [c]Universidad de Cantabria and CSIC (ES), [d]Belarussian State University (BY), [e]NIMP Bucharest-Magurele (RO)

37th RD50 Workshop
Zagreb – online Workshop
18.11 – 20.11.2020

Outline

Motivation

Radiation damages of LGADs
(Low Gain Avalanche Detectors) [1]:

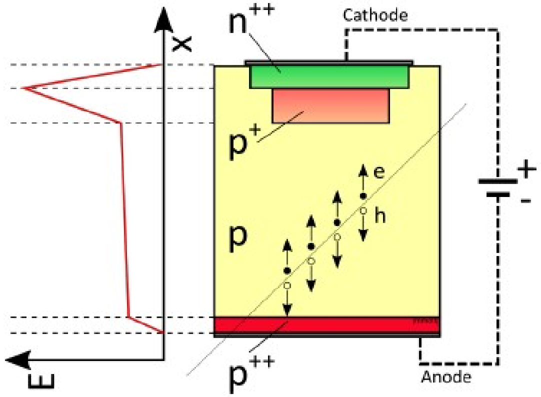

Fig 1. Schematic of LGAD

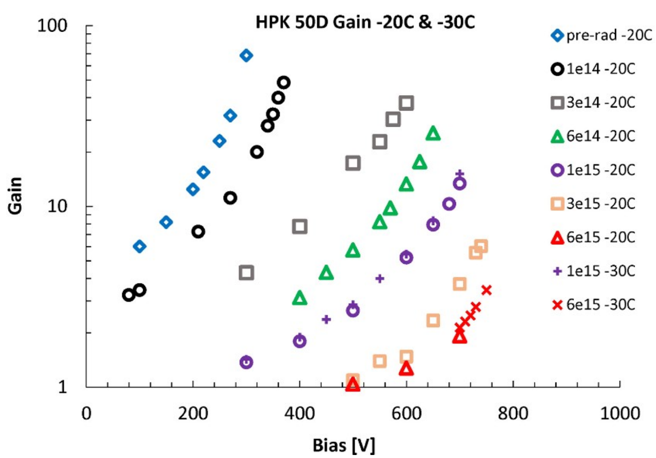

Fig 2. Gain value vs. bias for different fluence value

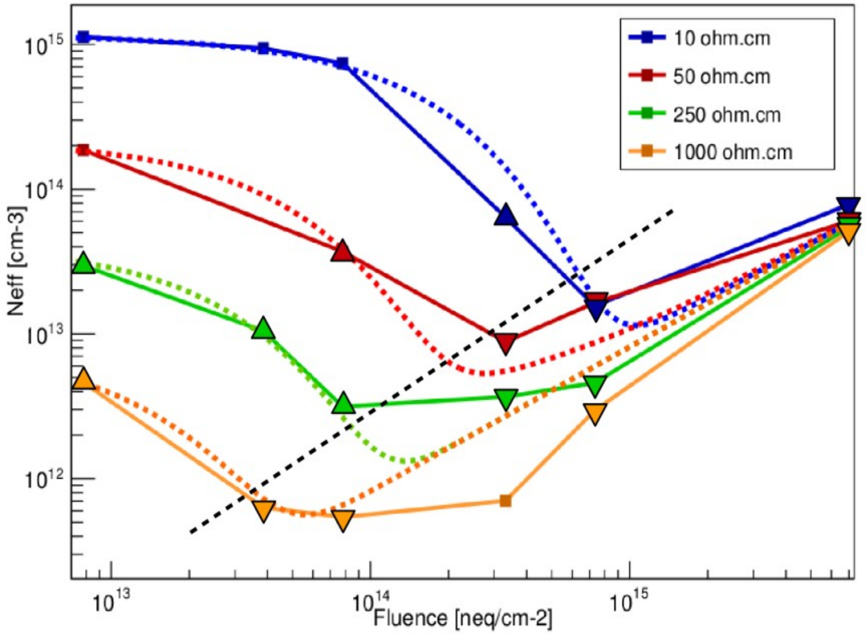

Fig 3. N_{eff} vs. fluence for different initial doping concentration

Radiation damage of p-type diodes is dominated by acceptor removal in the beginning and afterwords by acceptor generation.[2]

B^- turn to $B_iO_i^+$

Change in N_{eff} is a factor of 2

[1] Kramberger, G., et al. "Radiation effects in Low Gain Avalanche Detectors after hadron irradiations." Journal of Instrumentation 10.07 (2015): P07006.
[2] Y. Gurimskaya, 31st RD50 Workshop, 20-22 of November, 2017, CERN, Geneva, Switzerland.

Experimental details

Information of measured expitaxial silicon diodes (PIN)

Label	EPI50P_01_DS_73	EPI50P_06_DS_71	EPI50P_09_DS_73	EPI50P_12_DS_74
Resistivity	10 Ωcm	50 Ωcm	250 Ωcm	2000 Ωcm
Irradiation	23 GeV proton, Φ_{eq} = 4.28E13 cm^{-2}			
Area	6.927E-2 cm^2			
Thickness	50 µm			

C-V, I-V:

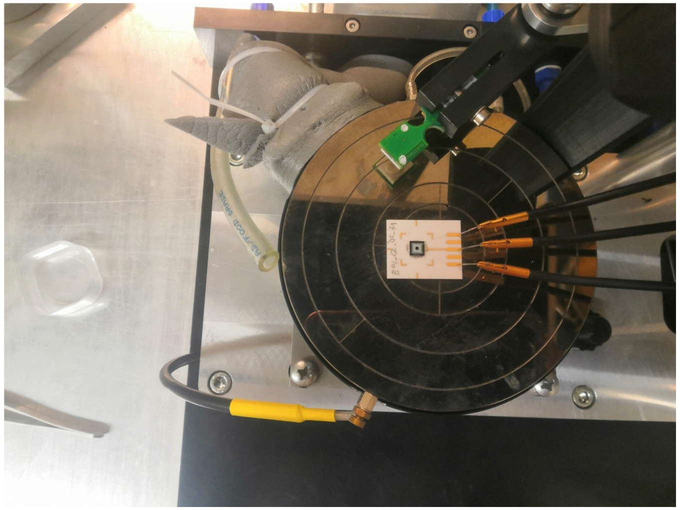

Experimental parameter (C-V, I-V):

Temperature: 20 °C
Humidity: below 10%
Frequency for C-V: 230 Hz, 455 Hz, 1k Hz, 10k Hz
AC voltage for C-V: 0.5 V

Thermally stimulated current-TSC:

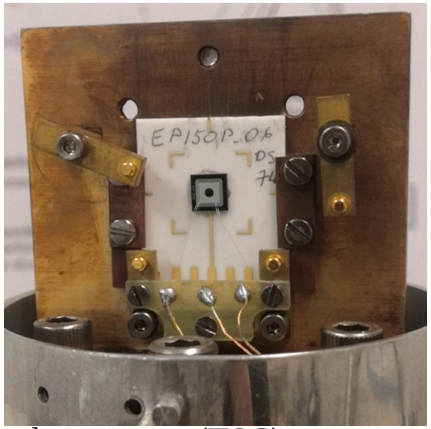

Experimental parameter (TSC):

Cooling down bias: 0 V
Filling temperature: typical 10 K
Filling: Forward bias filling, 0 V filling or light injection
Filling time: 30 s
Delay time: 30 s
Heating rate: 0.183 K/s
Heating up bias: depend on effective space charge concentration after irradiation

Experimental details

Basic Principle of Thermally Stimulated Current-(TSC) [2]:

a)

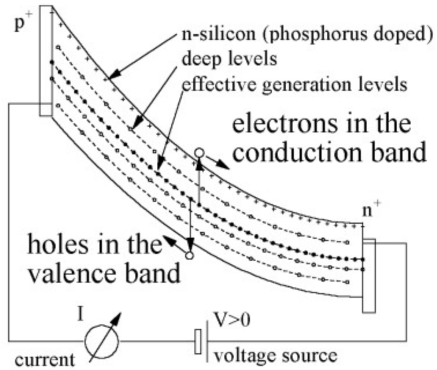

a) Cooling:
Room temperature → filling temperature

b)

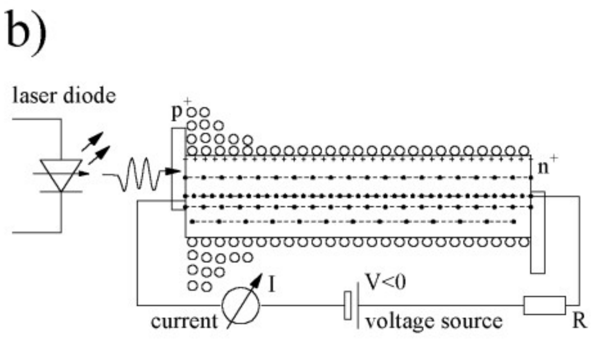

b) Injection:
Forward, 0 V or light injection

c)

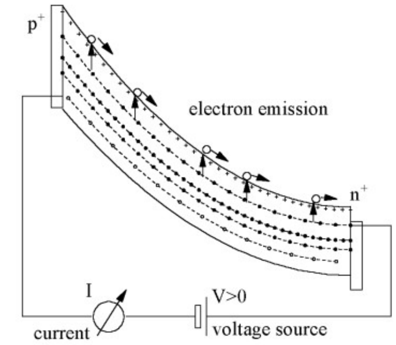

c) Heating up:
Reverse biased diodes, constant heating rate

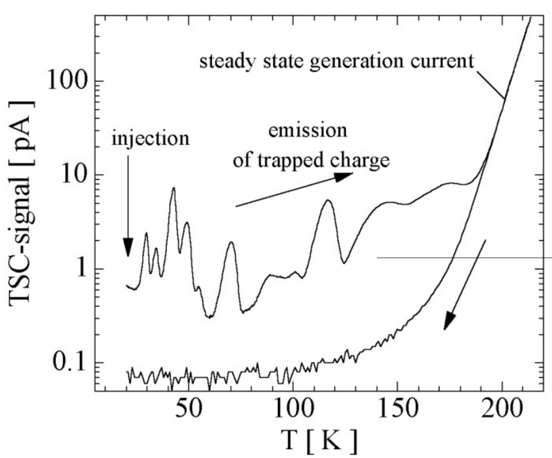

Fig 4. TSC spectrum [2]

$$I_{tsc}=\frac{1}{2}q_0\,A\,d(T)\,N_t\,e_n\exp\left(-\frac{1}{\beta}\int e_n(T)\,dT\right)$$

$$e_n=\sigma_n v_{th,n} N_c\times\exp\left(\frac{-E_a}{K_b T}\right)$$

$$E_a=E_C-E_T$$

[1]

N_t is defect concentration; β is heating rate; σ_n is capture cross section; E_a is activation energy; A is diodes area; d(T) depleted thickness;

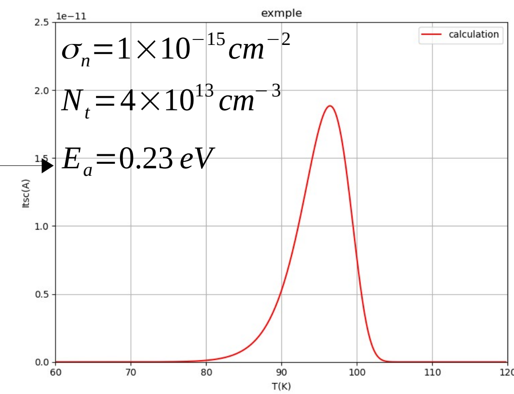

Fig 5. Example of calculated TSC peak

[1] Buehler, M. G. Solid-State Electronics 15.1 (1972): 69-79.
[2] Moll, Michael. No. DESY-THESIS-1999-040. DESY, 1999.

Example of TSC on B_iO_i(50 Ωcm)

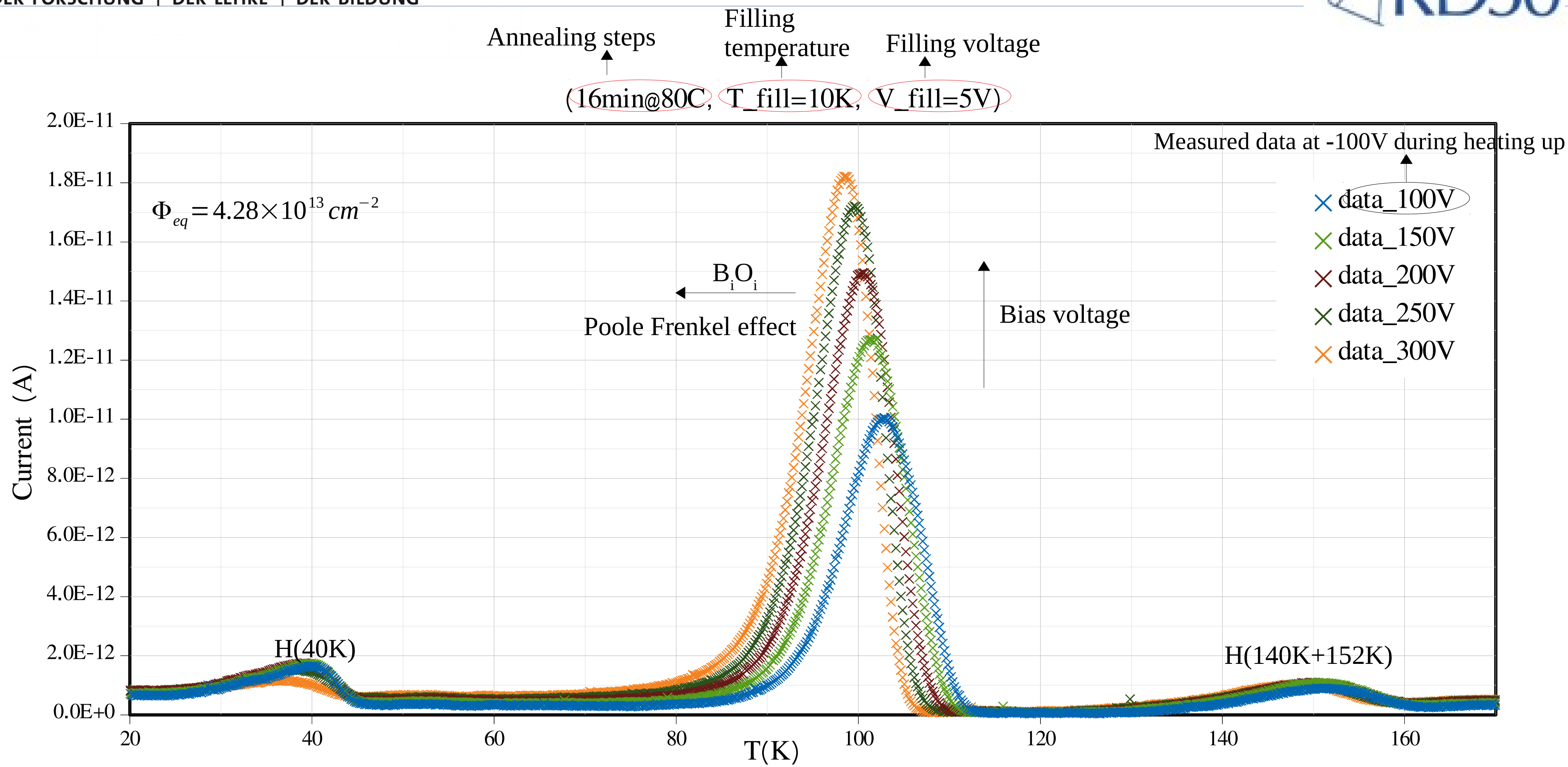

Fig 6. TSC spectra for different bias voltages of 50 Ωcm diode after 23 GeV proton irradiation

- Dominant B_iO_i signal
- Shift of peak maximum with V_{bias} → Poole-Frenkel effect; electron trap B_iO_i (o/+) donor defect
- Peak amplitude increases with bias voltage due to increasing depletion depth and after full depletion extending into the p+ region

Analysis method on B_iO_i(50 Ωcm)

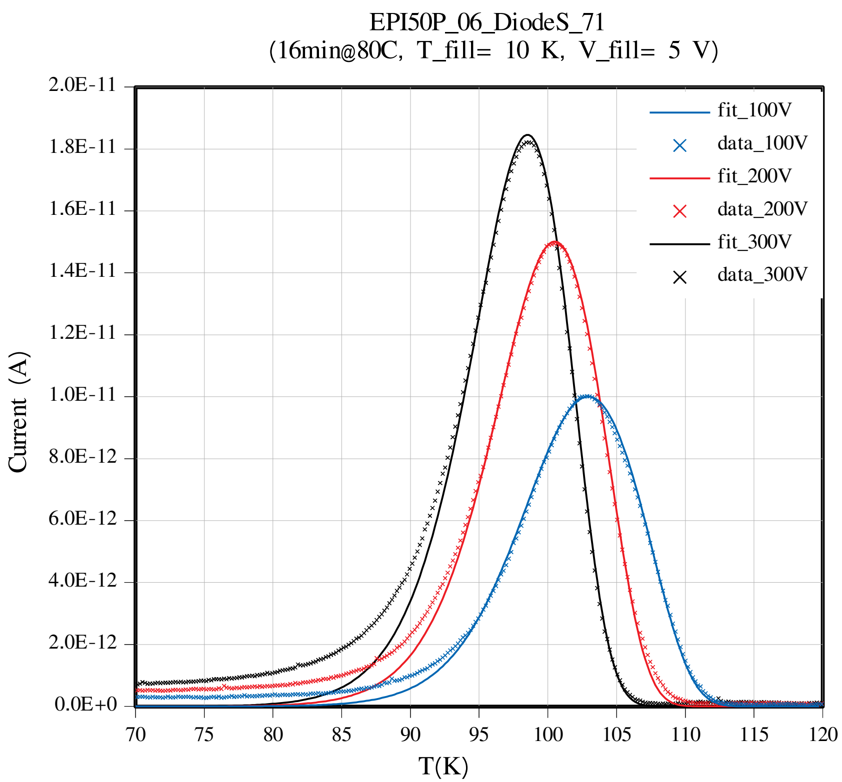

Fig 7. Results of fitting TSC Peak

Analysis method (3-D Poole Frankel effect) [1-3]:

$$I_{tsc}=\int_0^d \frac{1}{2} q_0 A x N_t e_n(T,x)\exp(-\frac{1}{\beta}\int e_n(T,x)dT)dx$$

$$e_n=\sigma_n v_{th,n} N_c \times \exp(\frac{-E_{a0}}{k_B T})[(\frac{1}{\gamma^2})(e^{\gamma}(\gamma-1)+1)+\frac{1}{2}]$$

$$\gamma=(\frac{q_0 E(x)}{\pi \varepsilon_0 \varepsilon_r})^{\frac{1}{2}} \times \frac{q_0}{k_B T}$$

q_0: elementary charge; A: area; d: depleted thickness; N_t: defect concentration; e_n: emission rate; T: temperature; x: position; β: heating rate; σ_n: electron captured cross section; $v_{th,n}$: thermal velocity of electron; N_C density of state in the conduction band; E_{a0}: zero field activation energy; k_B: Boltzmann constant; E(x): electric field.

[1] Buehler, M. G. Solid-State Electronics 15.1 (1972): 69-79.
[2] J. L. Hartke, J. Appl. Phys. 39, 4871 (1968).
[3] Pintilie, I., E. Fretwurst, and G. Lindström. Applied Physics Letters 92.2 (2008): 024101.

Annealing properties of B_iO_i(50 Ωcm)

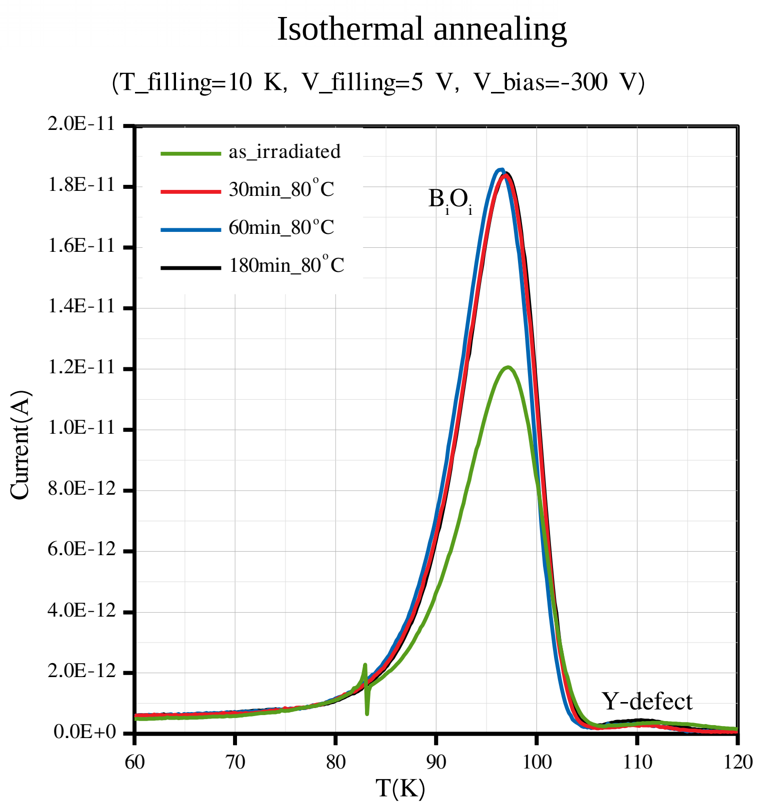

Fig 8. TSC for isothermal annealing

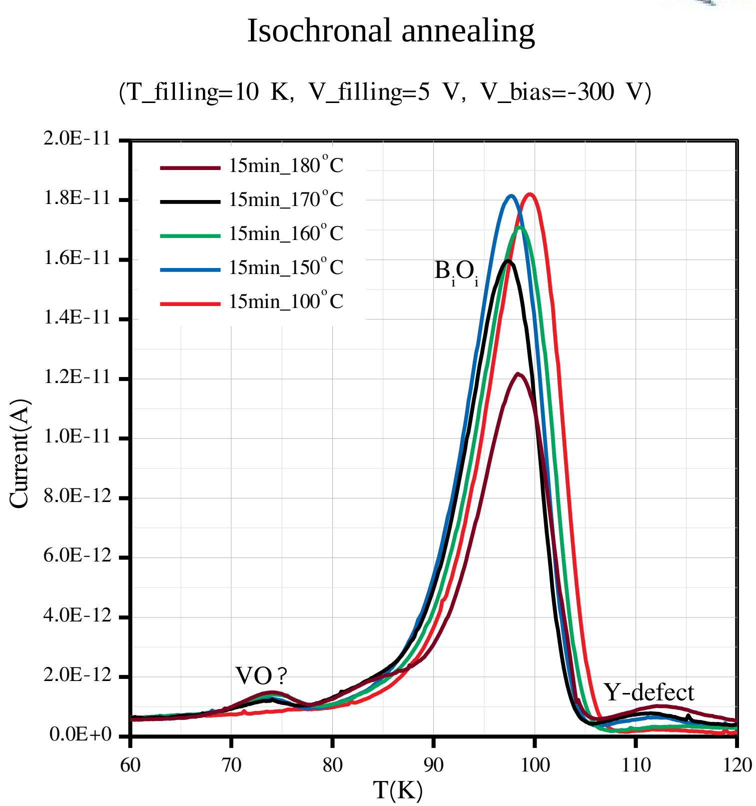

Fig 9. TSC for isochronal annealing

- B_iO_i increase after first annealing step and turn to stable during all annealing steps.

- B_iO_i is constant up to an annealing temperature of T_{ann} = 150 °C;
- For T_{ann} > 150 °C, [B_iO_i] decrease;
- Peak temperature slightly changes (unknown reason).
- Peak near B_iO_i at lower temperature range start to appear, possibly it is VO (didn't show Poole Frenkel effect).

Annealing properties of C-V(50 Ωcm)

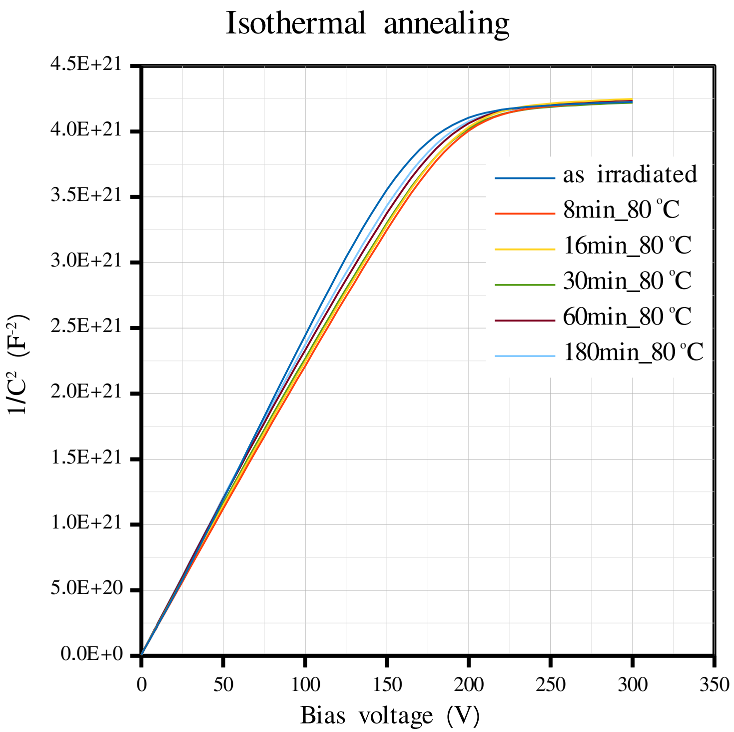

T=20 °C
Freq: 10 kHz
AC:0.5 V

$\Phi_{eq} = 4.28 \times 10^{13}\, cm^{-2}$

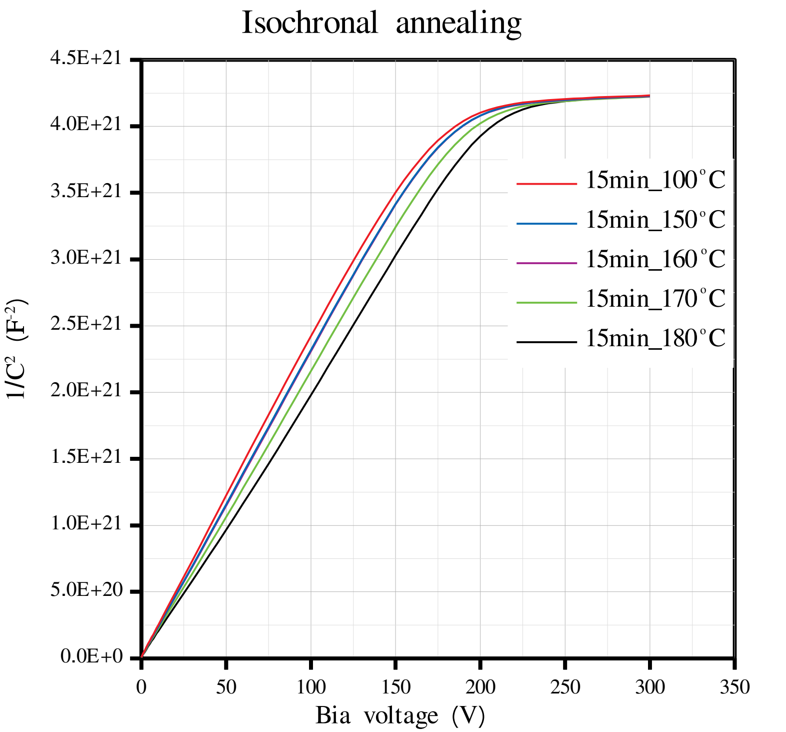

Fig 10. C-V for isothermal annealing at 80 °C up to 180 min

Fig 11. C-V curve for isochronal annealing steps (100 °C~ 180 °C)

Changes of capacitance are only small changes for different annealing steps due to most of shallow defects being nearly stable after annealing below 160 °C.

$[B_iO_i]$ and N_{eff} (C-V) for different annealing steps

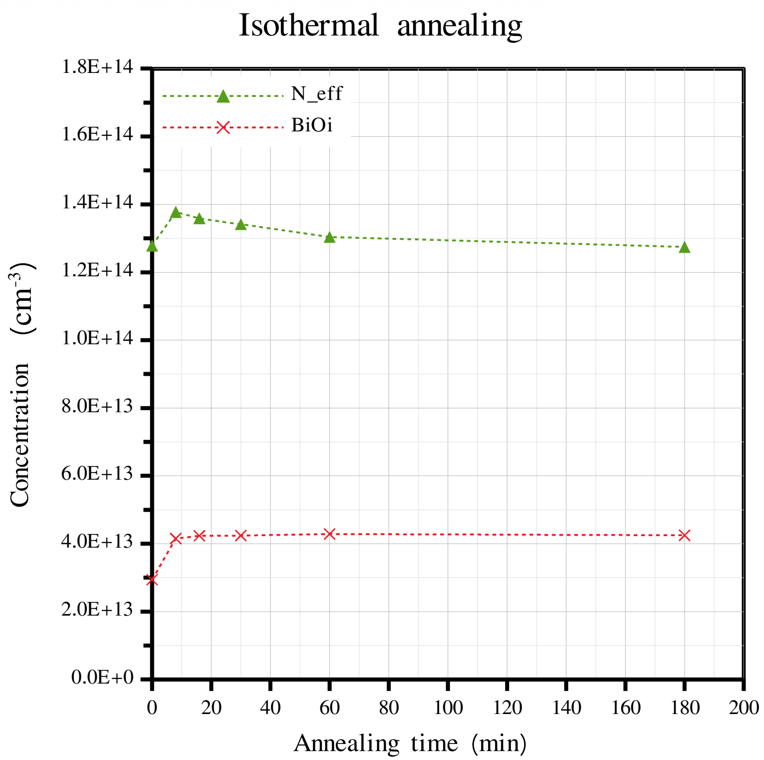

Fig 12. Concentration of B_iO_i and N_{eff} vs annealing time for isothermal annealing

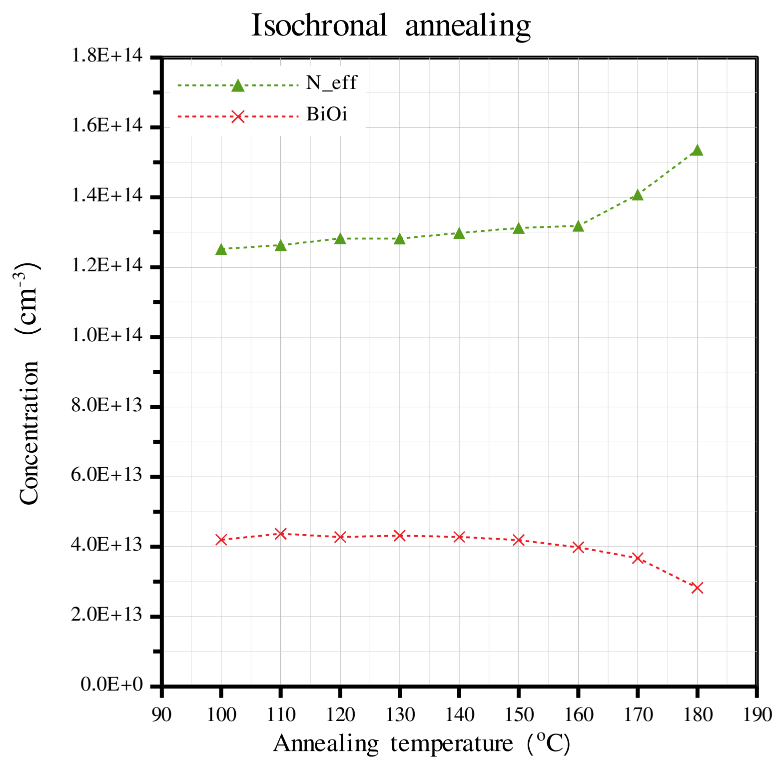

Fig 13. Concentration of B_iO_i and N_{eff} vs annealing temperature for isochronal annealing

$$N_{eff}(C-V)=N_s+2\times[B_iO_i]\pm others \qquad N_s=-[B_s]$$

- N_{eff} is given by C-V measurement;
- For isothermal annealing the change of N_{eff} is affected by defects(B_iO_i is constant);
- For isochronal annealing the change of N_{eff} is mainly affected by B_iO_i. And $N_{eff,\,180}-N_{eff,\,170} = 2\times([B_iO_i]_{170}-[B_iO_i]_{180})$.

Indication for X-defect(50 Ωcm)

16min@80C, V_filling=5 V, T_fill=60 K, V_bias=-250 V

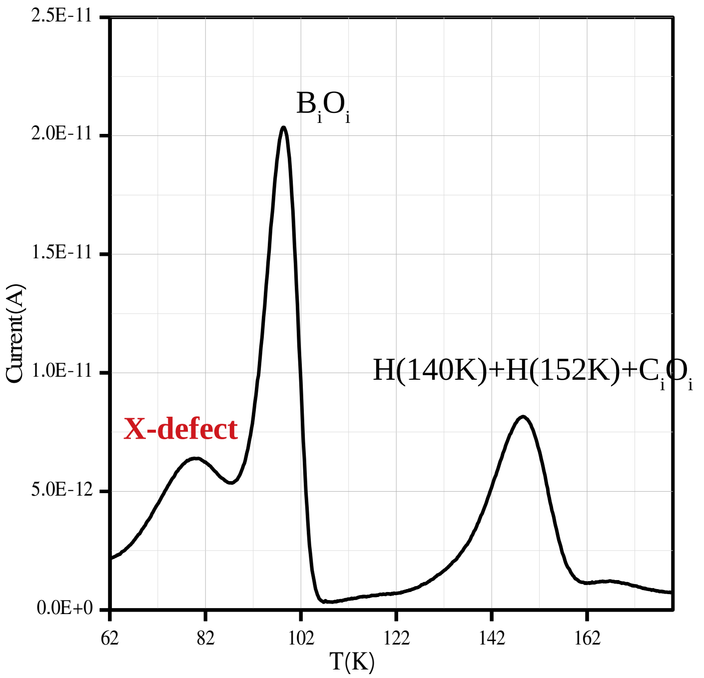

Fig 14. TSC spectrum of 50 Ωcm p-type diodes after filling at T_{fill} = 60 K with forwards bias V_{fill} = 5 V.

$$p_t = \frac{N_t}{\left(1+\frac{c_n}{c_p}\right)}$$

60min@80C, V_fill=0 V, T_fill=60 K, V_bias=-250 V

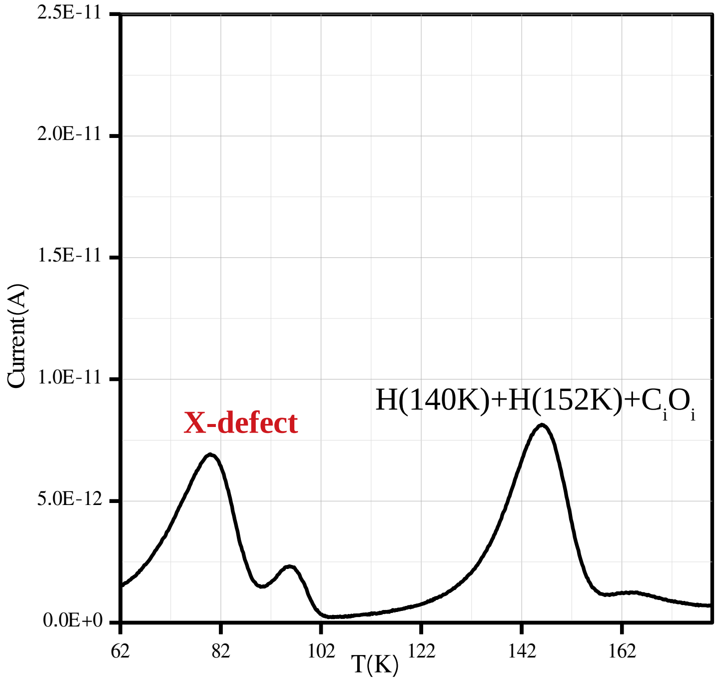

Fig 15. TSC spectrum for 0 V filling (majority carriers filling) and T_fill = 60 K

$$p_t = N_t\left(1-\exp\left(-c_p \cdot p \cdot t_{filling}\right)\right)$$

Compare two procedure:

- The capture cross section of X-defect is strongly temperature dependent
- X-defect is hole trap.

TSC spectra for 0 V filling(50 Ωcm)

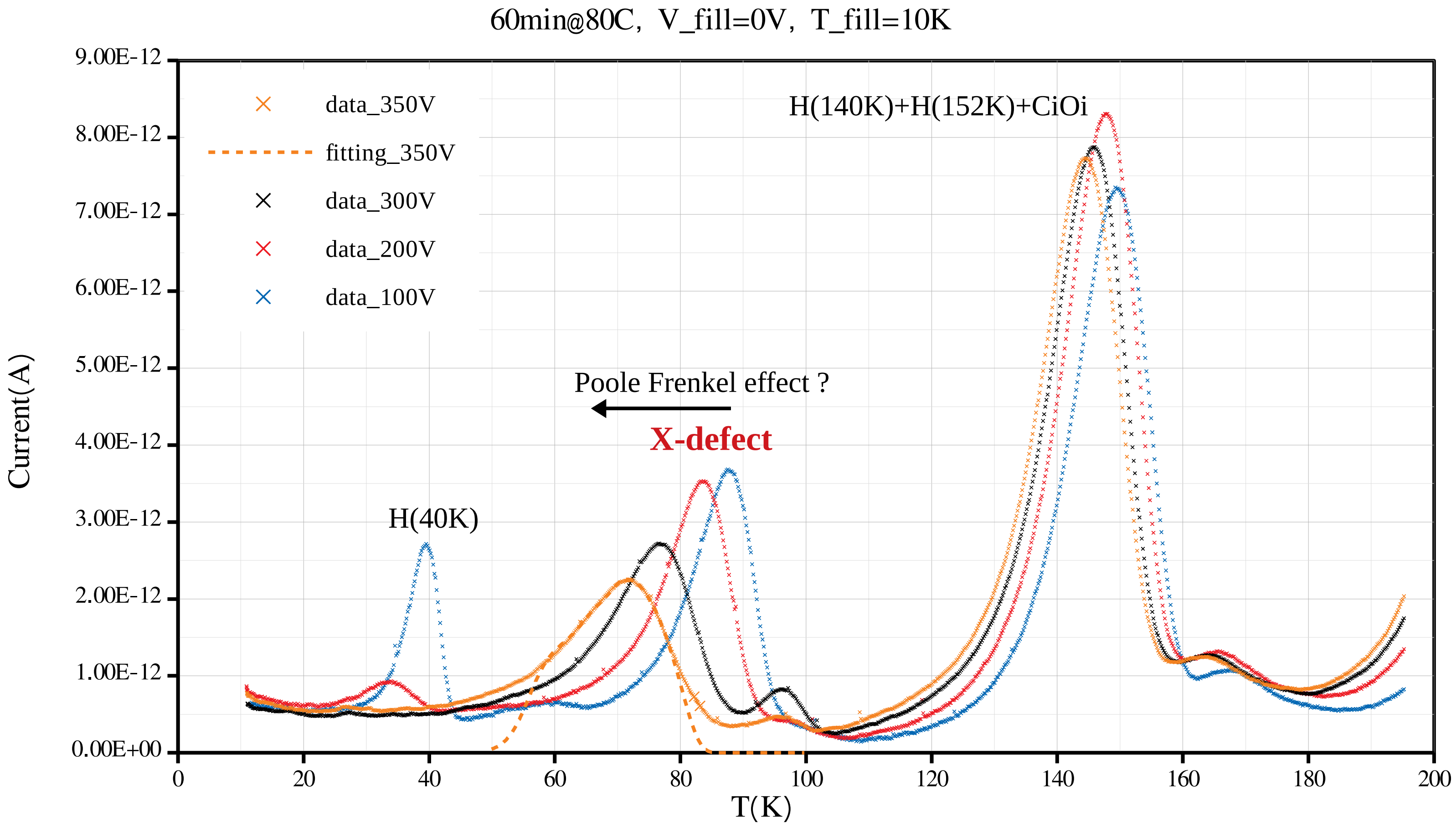

Fig 16. TSC spectra for different bias

- Special procedure: zero volt filling, only holes can be captured
- X-defect: hole trap, PF-effect, shallow acceptor → X(o/-), i.e. neutral if filled; T-shift very large ~ 15K for V_{bias} = 100~350 V. Long tail at higher bias voltage.
- $H(140K)+H(152K)+C_iO_i$: $E_t \approx E_V + 0.42eV$

Concentration of X-defect after isochronal annealing

50 Ωcm

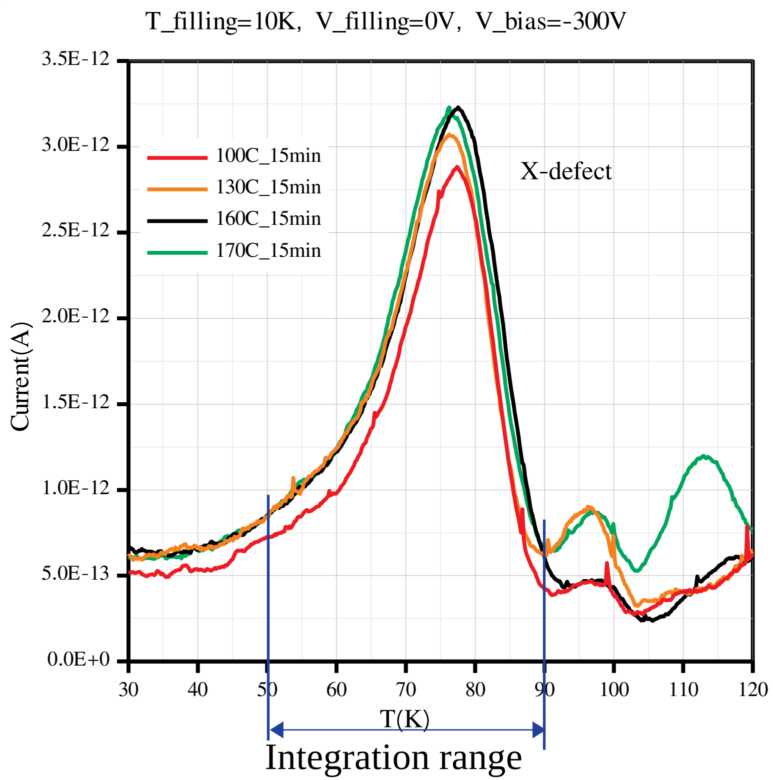

Fig 17. TSC spectra for 0 V filling and for different isochronal annealing steps

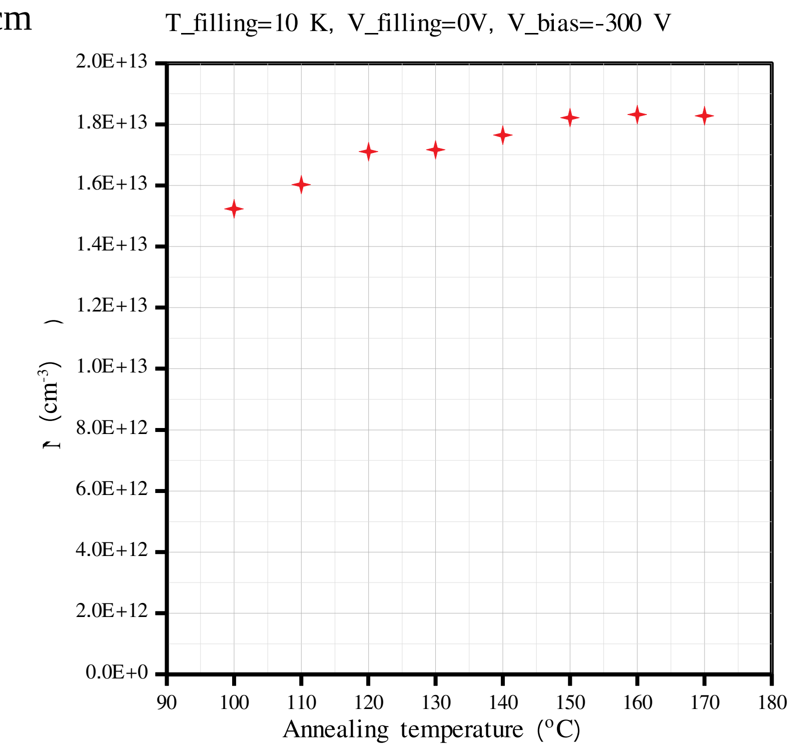

Fig 18. Defect concentration extracted from Fig 17 vs annealing temperature

$$N_t = \frac{2\int I\,dt}{q_0 A\, d(C)}$$

Concentration of X-defect slightly increases with annealing temperature

TSC spectra for diodes with different resistivity

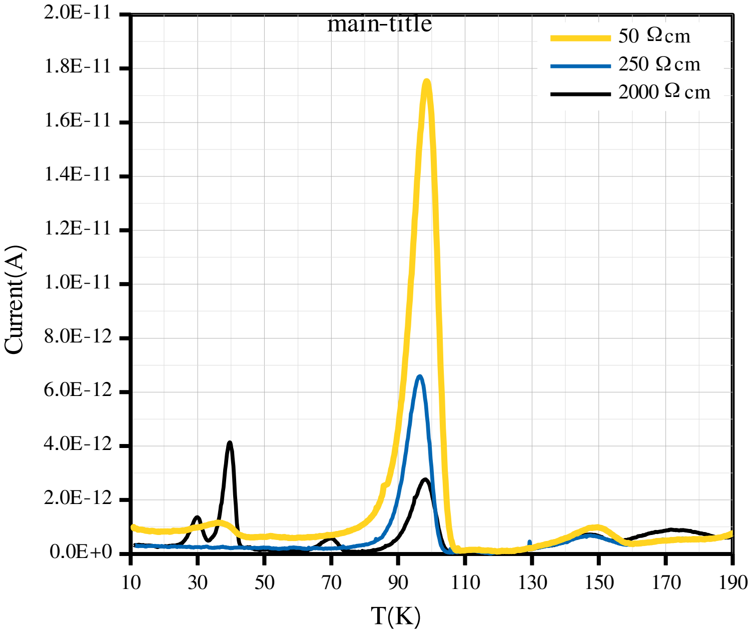

Fig 19. TSC spectra for diodes with different resistivity 50 Ωcm, 250 Ωcm and 2000 Ωcm

$\phi_{eq} = 4.28 \times 10^{13}\, cm^{-2}$

8min@80°C

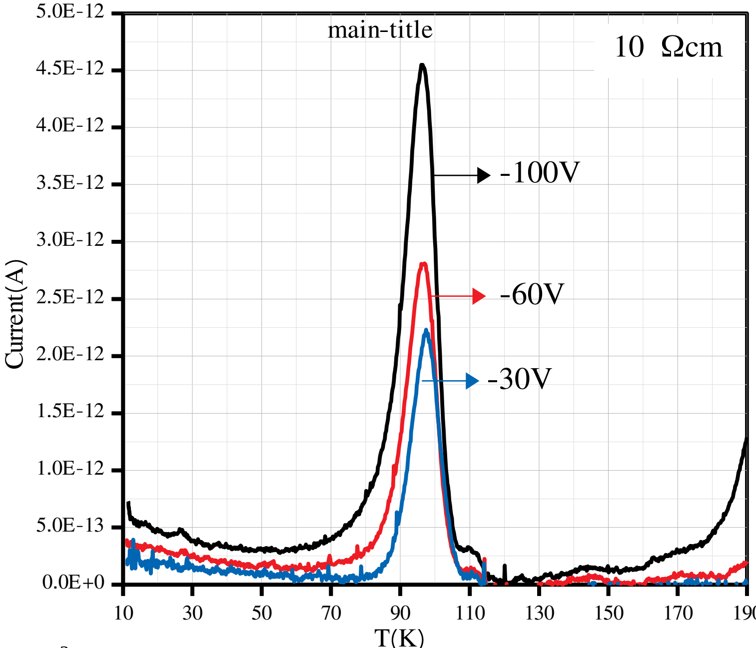

Fig 20. TSC spectra for 10 Ωcm diodes

Resistivity of measured diodes	V_{fill}	V_{bias}	T_{fill}	V_{fd} non-irradiation	V_{fd} (C-V)	Depleted depth(μm)
50 Ωcm	5V	-300V	10K	-372.0V	-180V	42.8
250 Ωcm	10V	-300V	10K	-74.4V	-20V	42.2
2000 Ωcm	10V	-100V	10K	-9.3V	-4V	41.8

Resistivity of measured diodes	V_{fill}	V_{bias}	T_{fill}	V_{fd} non-irradiation	V_{fd} (C-V)	Depleted depth(μm)
10 Ωcm	2V	-30V	10K	-1860.2V	-1674.2V	5.74
	2V	-60V	10K			8.03
	2V	-100V	10K			12.62

Introduction rate of B_iO_i for different doping

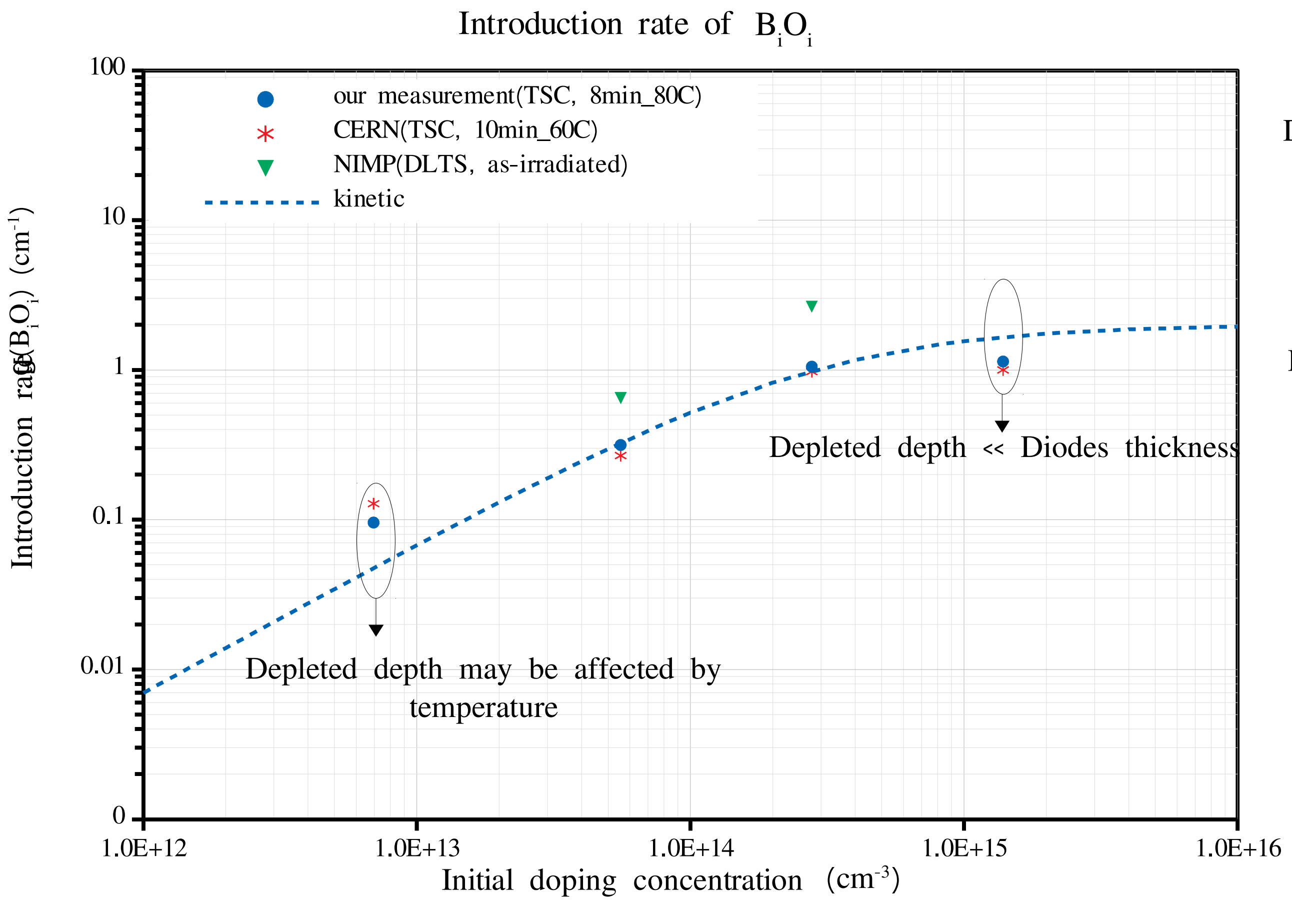

Fig 21. Introduction rate vs initial doping concentration

Definition of $g(B_iO_i)$:

$$g(B_iO_i)=\frac{N_{t,B_iO_i}}{\phi_{eq}}$$

Defect Kinetics Model [1-2]:

$$g(B_iO_i)\approx g_I\times\left(1+\frac{k_{IC}[C_s]}{k_{IB}[B_s]}\right)^{-1}$$

$$g_I\approx 2\,cm^{-1}$$

$$\frac{k_{IB}}{k_{IC}}\approx 7$$

$$[C_s]\approx 2\times 10^{15}\,cm^{-3}$$

For 250 and 2000 Ωcm, lowest defect concentration was used for calculated introduction rate (depleted depth range into the p+ region), defect concentration of 10 Ωcm given by average value of -30 V, -60 V and -100 V TSC measurements.

[1] Makarenko, Leonid F., et al. physica status solidi (a) 216.17 (2019): 1900354.
[2] Moll, Michael. "Acceptor removal-Displacement damage effects involving the shallow acceptor doping of p-type silicon devices." (2019).

Summary

I. B_iO_i defect for 50 Ωcm diodes irradiated with 23 GeV protons

Describe B_iO_i peak on TSC spectra:

3-D Poole Frenkel effect (shift with bias voltage)

Annealing behaviors:

Isothermal annealing 80 °C:

- B_iO_i is stable

Isochronal annealing:

- If T_{ann} > 150 °C, [B_iO_i] decrease
- T_{ann} = 170 °C and T_{ann} = 180 °C shows that the change $\Delta N_{eff} \approx 2 \times \Delta N_t$ (B_iO_i) as expected from $B_s(-) \rightarrow B_iO_i (+)$

II. X-defect:

- Hole trap, shift with bias voltage, a long tail at T below T_{max}
- After isochronal annealing, X-defect slightly increases
- Temperature dependent capture cross section of holes

III. Measurements for diodes with different resistivity :

- V_{fd} after irradiation to $\Phi_{eq} = 4.28 \times 10^{13}$ cm^{-2} significantly decrease for high resistivity material (50 Ωcm, 250 Ωcm, 2k Ωcm).
- Higher initial doping concentration leads to higher B_iO_i introduction rate after the same fluence value. But the increase is not linear .

Further plan : the degradation of the gain in LGAD device seems to be dominated by the boron removal in the gain layer. This has to be validated microscopic studied on irradiated LGADs.